Versatile waveguide-coupled optofluidic devices based on liquid core optical ring resonators

Ian M. White, John Gohring, Yuze Sun, Gilmo Yang, Scott Lacey, and Xudong Fan[a)]
Department of Biological Engineering, University of Missouri—Columbia, 240D Bond Life Sciences Center, 1201 E. Rollins Street, Columbia, Missouri 65211, USA

(Received 21 September 2007; accepted 24 November 2007; published online 10 December 2007)

A versatile waveguide-coupled optofluidic device using the liquid core optical ring resonator (LCORR) that can be operated with liquid of any refractive index (RI) is theoretically analyzed and experimentally demonstrated. The results confirm the confinement of resonant modes for all sample RIs, and reveal that confined modes in a high-RI core are excited by an external waveguide by resonant tunneling through the LCORR wall. It is further found that a thin wall must be used for effective interaction between the core mode and the waveguide. The results have important applications in optofluidic devices, including sensors, microfluidic lasers, and nonlinear optics.
 [DOI: 10.1063/1.2824843]

Integrating optical ring resonators with fluidics is an important research area in optofluidics.[1,2] Such integration permits efficient delivery of liquid samples and control of the light in the whispering gallery modes (WGMs) through fluids, which has broad applications in bio/chemical sensors,[3–5] microfluidic lasers,[6–8] optical components,[9] nonlinear optics,[10] and cavity QED.[11] Microdroplets as an optofluidic ring resonator (OFRR) have been extensively studied and utilized in the past decades,[6,10,12] but they suffer from evaporation and are difficult to integrate with other components. Alternatively, optofluidic devices such as sensors, lasers, and frequency-tunable devices have been achieved with solid-state ring resonators immersed in a liquid chamber.[3–5,8,9] However, in those OFRRs, the fluidics has to be fabricated separately and then mounted onto ring resonators through multiple steps, which may present many design challenges. More importantly, as the refractive index (RI) of the liquid medium approaches the ring resonator's RI, the radiative loss of the WGM increases tremendously, due to the reduced RI contrast [Fig. 1(a)], severely spoiling the Q factor of the resonator. This significantly limits the liquids that can be used in typical OFRRs, especially in ring resonators based on fused silica, which have extremely high Q factors, but relatively low RI ($n=1.45$).

We recently introduced another type of OFRR, the liquid core optical ring resonator (LCORR) based on a thin-walled glass capillary [Fig. 1(b)], which inherently integrates the ring resonator with microfluidics.[13–15] Intuitively, when the RI of the liquid core is lower than that of the capillary wall, the circular cross section of the capillary wall forms the ring resonator; the WGM is mainly confined in the wall and interacts with the liquid sample in the core via the evanescent field, as shown theoretically and experimentally in Ref. 13. More recently, refractometric sensing and microfluidic lasers have been demonstrated when the RI of the liquid core is higher than that of the capillary wall.[16–18] Therefore, it is of importance to understand the operational principle of this system in order to realize its full potential as an optofluidic device. In this letter, we explore the versatility of the LCORR in handling liquids in the core. We show that when the core's RI exceeds that of the wall, WGMs form at the LCORR inner surface, in addition to the WGMs bound by the capillary outer surface. We further show that the WGMs interact not only with the liquid core, but also with the waveguide outside the LCORR (even when the core RI is much higher than that of the wall), thus enabling optical interrogation of the liquid samples in the core for sensing, excitation or outcoupling of the emissions from the liquid samples, and fluidic control of the optical signal transmitted in the waveguide.

The WGM of the LCORR can be analyzed using the analog of a quantum mechanical potential well.[19] The total energy of the wave is k^2 ($k=2\pi/\lambda$, where λ is the WGM wavelength in vacuum) and the potential is defined as $V(r)=k^2(1-n^2)+l^2/r^2$, where n is the RI, l is the angular momentum term, and r is the radial position. Figure 2 shows the evolution of a particular WGM for a silica LCORR with liquid core RIs of 1.33, 1.45, 1.5, and 1.6. The WGM spectral position and mode profile are calculated using a three-layer Mie scattering model.[13] As expected, with $n_{core}=1.33$ [Fig. 2(a)], an evanescent field exists both inside and outside the LCORR, which enables the WGM excitation through a waveguide and the interaction with the liquid sample in the core, as demonstrated previously.[13–15] When n_{core} is increased to 1.45 [Fig. 2(b)], the LCORR essentially becomes equivalent to a solid silica cylinder ring resonator and more light is pulled into the core.

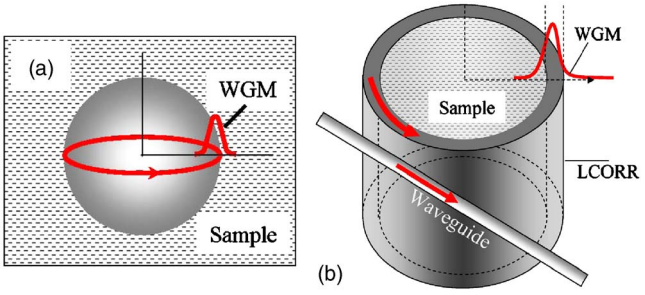

FIG. 1. (Color online) (a) In a microsphere, the WGMs are bound at the interface of the liquid sample and the sphere surface. (b) In the LCORR, the WGMs form at the wall/air boundary or at the liquid/wall boundary.

[a)]Author to whom correspondence should be addressed. Electronic mail: fanxud@missouri.edu

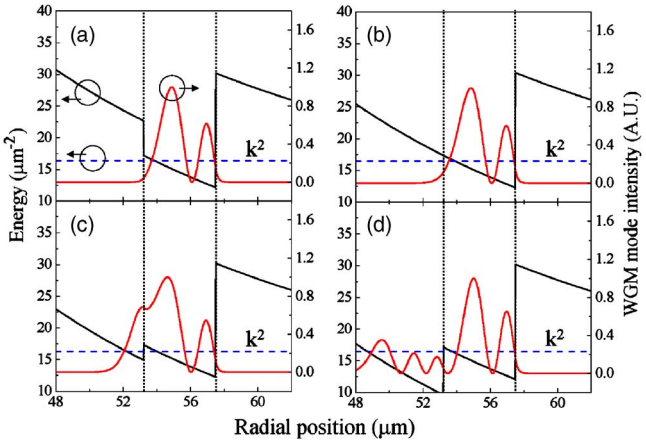

FIG. 2. (Color online) Potential well formed by the core and the LCORR wall, and the WGM radial mode profile for (a) $n_{core}=1.33$, $\lambda=1.552\,933\,2\ \mu m$; (b) $n_{core}=1.45$, $\lambda=1.553\,937\,2\ \mu m$; (c) $n_{core}=1.5$, $\lambda=1.55\,7271\,0\ \mu m$; (d) $n_{core}=1.6$, $\lambda=1.549\,423\,0\ \mu m$. All cases are TE mode, $l=316$, $R=57.5\ \mu m$, $t=4.3\ \mu m$, $n_{wall}=1.45$. Vertical dashed lines indicate the inner and outer surface of the LCORR. Horizontal dashed lines are the values for k^2. Fraction of the total optical mode intensity that exists outside the glass wall $\eta_{outside}$: (a) 0.93%, (b) 0.86%, (c) 0.55%, and (d) 0.79%.

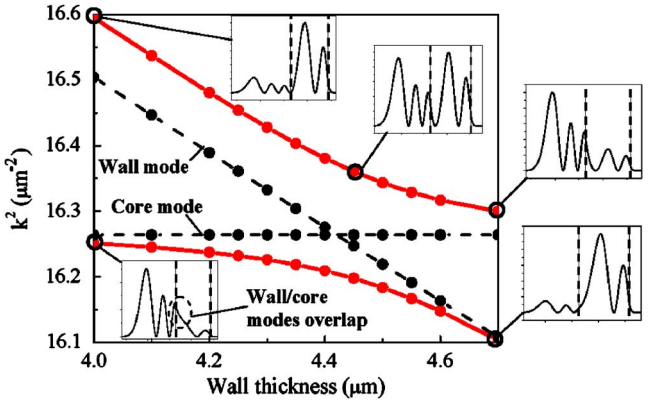

FIG. 3. (Color online) Dispersion diagram showing the existence of bonding and antibonding modes due to the interaction of the WGMs in the liquid core and glass wall. Increasing wall thickness implies that the ID is constant and the OD increases. Parameters: TE mode, $l=316$, inner radius $=53.2\ \mu m$, $n_{wall}=1.45$, and $n_{core}=1.6$. Dashed lines represent WGM in glass wall assuming the absence of the WGM in the core and vice versa. The wall mode is calculated by setting $n_{core}=1.45$ (eliminates core mode); the core mode is calculated by setting $n_{outside}=1.45$ (eliminates wall mode).

As the RI of the liquid core increases above that of the LCORR [Figs. 2(c) and 2(d)], two bound potential wells emerge at the wall/air boundary and at the liquid/wall boundary, respectively. For the given wall thickness, these two potential wells are close enough in proximity so that the WGMs in these two wells interact strongly. Figure 2(d) shows that the third order WGM in the core interacts with the second order WGM in the LCORR for the given parameters. The two modes form bonding and antibonding modes, which is shown by the dispersion diagram and the bonding and antibonding mode structures presented in Fig. 3 [using the parameters from Fig. 2(d)]. The formation of bonding and antibonding modes has also been analyzed recently for a microsphere in an effort to establish photonic molecules.[20] In the case of the LCORR, the formation of the bonding and antibonding WGMs significantly promotes the coupling between the WGM originally in the liquid and the waveguide that is separated by a silica gap of a few micrometers. This coupling can also be interpreted as resonant tunneling of the WGM through the potential well formed by the LCORR wall. Detailed analysis shows that the fraction of the evanescent light outside the LCORR is between 0.5% and 1% in all four RIs, which yields a sufficient field overlap between the WGM and the waveguide.[14,21,22]

Phase mismatch must also be considered to completely describe the coupling between the ring resonator and waveguide. We can use the LCORR/waveguide coupling analysis presented in Ref. 23, where the overlap integrals are calculated using the waveforms in Fig. 2 and the phase mismatch is calculated from the difference in propagation constant $\Delta\beta$, where $\Delta\beta=\beta_{WGM}-\beta_{waveguide}$ and $\beta_{WGM}=l/R$. Using the parameters of Fig. 2 and a taper with a 3 μm diameter, $\beta_{WGM}=6.0$ and $\beta_{waveguide}=5.63$. For the extreme case of a core RI of 1.6, we calculate a coupling coefficient $\kappa^2=1.5\times10^{-3}$, which is sufficient for efficient coupling.

It should be emphasized that a thin wall is necessary for a waveguide-coupled system. As the wall becomes thicker, the WGMs in the core start to de-couple with the waveguide. This decoupling is not caused by the diminishing evanescent field outside the LCORR, as the fraction of the light remains

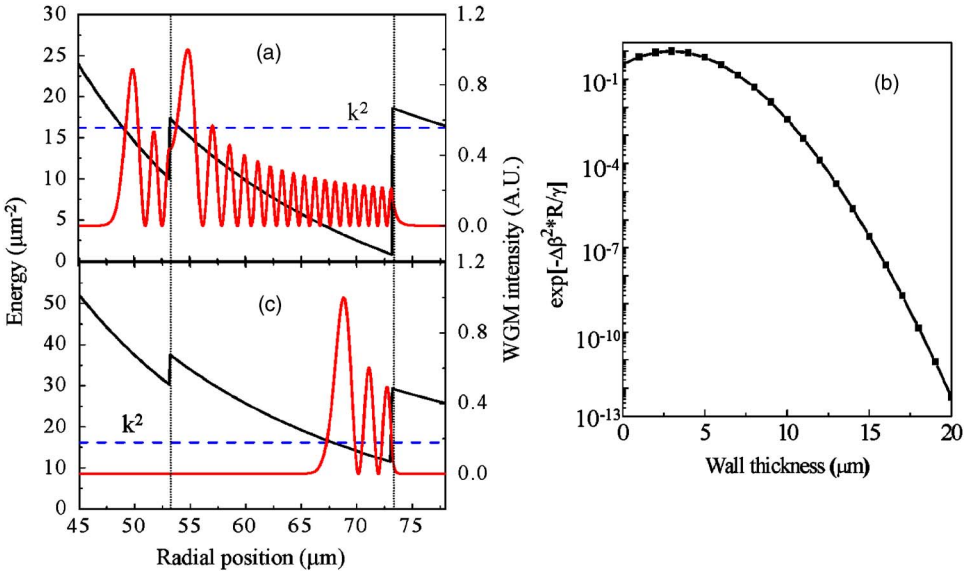

FIG. 4. (Color online) (a) Potential well and the WGM radial mode profile in a silica LCORR with $R=73.2\ \mu m$ and wall thickness$=20\ \mu m$. $n_{core}=1.6$, $\lambda=1.560\,297\ \mu m$, $l=316$, TE mode, and $\eta_{outside}=1\%$. (b) Impact of wall thickness on waveguide/LCORR coupling. $l=316$, $R=53.2\ \mu m+$wall thickness, $\beta_{waveguide}=5.63\ \mu m^{-1}$ for a 3 μm diameter taper. (c) Potential well and WGM for $n_{core}=1.6$, $\lambda=1.559\,979\ \mu m$, $l=396$, TE mode, and $\eta_{outside}=0.71\%$. Horizontal dashed lines in (a) and (c) are the values for k^2.

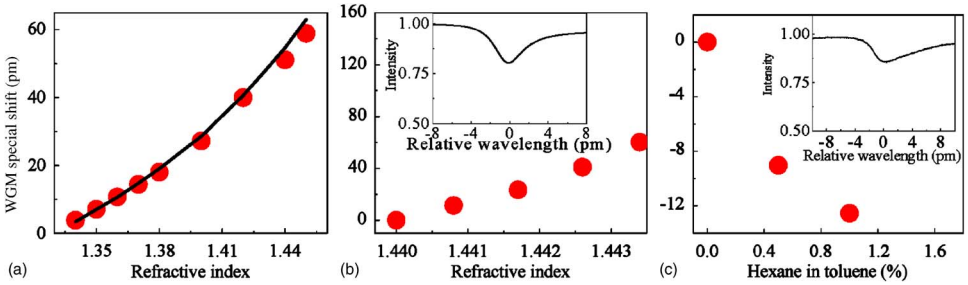

FIG. 5. (Color online) (a) Measured (circle) and calculated (solid line) spectral shift of the WGM as the liquid core RI increases. $R=57.5$ μm, $t=5.3$ μm, $l=317$, and TE mode. (b) Measured spectral shift as the liquid core RI increases. Inset: recorded WGM at $n_{core}=1.444$. (c) Measured spectral shift as the percentage of hexane in toluene increases. Inset: recorded WGM at $n_{core}=1.5$.

more or less constant [see Fig. 4(a)], but rather by the drastic decrease in coupling strength due to large phase mismatch between the WGM and the waveguide [Fig. 4(b)], which is proportional to $\exp(-\Delta\beta^2 R/\gamma)$, where γ is the decay constant of the LCORR evanescent field, approximated as $\gamma = k\sqrt{n_{wall}^2 - 1}$.[14] Note that as the wall becomes thicker, the potential well from the LCORR wall becomes deeper and lower energy WGMs emerge, as shown in Fig. 4(c). These low-lying WGMs do not interact with the WGM in the core due to the large spatial and energetic separation, and thus cannot be employed to mediate the interaction between the liquid sample and the waveguide. Based on the change in $\Delta\beta^2$ shown in Fig. 4(b), the κ^2 is many orders of magnitude lower. For thick-walled capillaries, a prism may be used to reduce the phase mismatch and to reach the WGM in the liquid core at the expense of convenient light guiding and system integration of the waveguide.[24]

We experimentally validate the LCORR's RI versatility and show that the interaction between the WGM and the waveguide can be maintained over a wide range of liquid RIs by performing refractometric sensing demonstrations using two silica LCORRs and liquids with RI varying from 1.33 to 1.5. A 1550 nm tunable diode laser is coupled into a fiber taper of 3 μm in diameter in touch with the LCORR to excite the WGM. The details related to the LCORR fabrication, wall thickness characterization, and the experimental setup for refractometric sensing with the LCORR have been described elsewhere.[13,15] We first use the LCORR with the thicker wall ($t=5.34$ μm), which has a low RI sensitivity, so that a wide range of RI can be observed. The shift of one particular WGM is tracked continuously as solutions of sucrose in water with the RI ranging from 1.33 to 1.45 are flowed through the LCORR, as shown in Fig. 5(a). The data are in excellent agreement with the theoretical calculation. To observe small RI changes, in Fig. 5(b) we use the second LCORR ($t=4.3$ μm, which is the value used in the theoretical analysis) with higher sensitivity. The LCORR can still operate as a waveguide-coupled optofluidic device, even when the liquid core has a higher RI than the LCORR material. In Fig. 5(c), the second LCORR is filled with toluene ($n=1.5$), which corresponds to the case analyzed in Fig. 2(c). When toluene-hexane mixture is passed through, the WGM shifts to a lower wavelength due to a lower RI of hexane ($n=1.375$).

In summary, the versatility of operation of a waveguide-coupled LCORR has been demonstrated. Theoretical analysis shows that waveguide-coupled operation at high RI is still possible because the WGM in the LCORR wall and the WGM in the high-RI core are interacting. This is verified by observing through the analysis that these modes create bonding and antibonding modes. Furthermore, coupling analysis shows that a thin wall is critical for operation, even at high RI, to satisfy the phase matching condition. Future work on the LCORR will focus on the realization of waveguide-coupled optofluidic lasers using a wide range of solvent RIs.[18] Beyond this, nonlinear optical phenomena such as two-photon fluorescence and Raman scattering will be investigated. Liquid tuning of the WGM to achieve critical coupling with the waveguide will also be explored. The LCORR is also a potential model system for realization of previously proposed photonic molecules.[20]

This work is sponsored by the Wallace H. Coulter Foundation and the NIH (1K25 EB006011). Two of the authors (G.Y. and S.L.) are visiting scholars from South Korea National Institute of Agricultural Engineering and Franklin & Marshall College, respectively.

[1] C. Monat, P. Domachuk, and B. J. Eggleton, Nat. Photonics **1**, 106 (2007).
[2] D. Psaltis, S. R. Quake, and C. Yang, Nature (London) **442**, 381 (2006).
[3] F. Vollmer, D. Braun, A. Libchaber, M. Khoshsima, I. Teraoka, and S. Arnold, Appl. Phys. Lett. **80**, 4057 (2002).
[4] N. M. Hanumegowda, C. J. Stica, B. C. Patel, I. M. White, and X. Fan, Appl. Phys. Lett. **87**, 201107 (2005).
[5] K. D. Vos, I. Bartolozzi, E. Schacht, P. Bienstman, and R. Baets, Opt. Express **15**, 7610 (2007).
[6] H.-M. Tzeng, K. F. Wall, M. B. Long, and R. K. Chang, Opt. Lett. **9**, 499 (1984).
[7] S. I. Shopova, H. Zhu, X. Fan, and P. Zhang, Appl. Phys. Lett. **90**, 221101 (2007).
[8] H.-J. Moon, Y.-T. Chough, and K. An, Phys. Rev. Lett. **85**, 3161 (2000).
[9] U. Levy, K. Campbell, A. Groismanb, S. Mookherjea, and Y. Fainman, Appl. Phys. Lett. **88**, 111107 (2006).
[10] A. S. Kwok and R. K. Chang, Opt. Lett. **18**, 1703 (1993).
[11] R. K. Chang and A. J. Campillo, *Optical Processes in Microcavities* (World Scientific, Singapore, 1996).
[12] M. Hossein-Zadeh and K. J. Vahala, Opt. Express **14**, 10800 (2006).
[13] I. M. White, H. Oveys, and X. Fan, Opt. Lett. **31**, 1319 (2006).
[14] I. M. White, H. Oveys, X. Fan, T. L. Smith, and J. Zhang, Appl. Phys. Lett. **89**, 191106 (2006).
[15] X. Fan, I. M. White, H. Zhu, J. D. Suter, and H. Oveys, Proc. SPIE **6452**, 6452 (2007).
[16] V. Zamora, A. Diez, M. V. Andres, and B. Gimeno, Opt. Express **15**, 12011 (2007).
[17] M. Sumetsky, R. S. Windeler, Y. Dulashko, and X. Fan, Opt. Express **15**, 14376 (2007).
[18] S. Lacey, I. M. White, Y. Sun, S. I. Shopova, J. M. Cupps, P. Zhang, and X. Fan, Opt. Express **15**, 15523 (2007).
[19] B. R. Johnson, J. Opt. Soc. Am. A **10**, 343 (1993).
[20] I. Teraoka and S. Arnold, Opt. Lett. **32**, 1147 (2007).
[21] J. C. Knight, G. Cheung, F. Jacques, and T. A. Birks, Opt. Lett. **22**, 1129 (1997).
[22] M. L. Gorodetsky and V. S. Ilchenko, J. Opt. Soc. Am. B **16**, 147 (1999).
[23] I. M. White, H. Oveys, X. Fan, T. Smith, and J. Zhang, Appl. Phys. Lett. **89**, 191106 (2006).
[24] T. Ling and L. J. Guo, Opt. Express (in press).